Investigation of the near-threshold cluster resonance in ^{14}C*

Hong-Liang Zang(臧宏亮)[1] Yan-Lin Ye(叶沿林)[1;1)] Zhi-Huan Li(李智焕)[1] Jian-Song Wang(王建松)[2]
Jian-Ling Lou(楼建玲)[1] Qi-Te Li(李奇特)[1] Yu-Cheng Ge(葛愉成)[1] Xiao-Fei Yang(杨晓菲)[1]
Jing Li(李晶)[3] Wei Jiang(蒋伟)[4] Jun Feng(冯俊)[1] Qiang Liu(刘强)[1] Biao Yang(杨彪)[1]
Zhi-Qiang Chen(陈志强)[1] Yang Liu(刘洋)[1] Hong-Yi Wu(吴鸿毅)[1] Chen-Yang Niu(牛晨阳)[1]
Chen-Guang Li(李晨光)[1] Chun-Guang Wang(王春光)[1] Xiang Wang(王翔)[1] Wei Liu(刘威)[1]
Jian Gao(高见)[1,5] Han-Zhou Yu(余翰舟)[1] Jun-Bin Ma(马军兵)[2] Peng Ma(马朋)[2] Zhen Bai(白真)[2]
Yan-Yun Yang(杨彦云)[2] Shi-Lun Jin(金仕纶)[2] Fei Lu(卢飞)[6]

[1] School of Physics and State Key Laboratory of Nuclear Physics and Technology, Peking University, Beijing 100871, China
[2] Institute of Modern Physics, Chinese Academy of Science, Lanzhou 730000, China
[3] Argonne National Laboratory, 9700 S Cass Ave B109, Lemont, Illinois 60439, USA
[4] Institute of High Energy Physics, CAS, Beijing 100049, China
[5] RIKEN Nishina Center, 2-1 Hirosawa, Wako, Saitama 351-0198, Japan
[6] Shanghai Institute of Applied Physics, Chinese Academy of Science, Shanghai 200000, China

Abstract: An experiment for p(^{14}C,^{14}C* $\rightarrow^{10}$ Be+α)p inelastic excitation and decay was performed in inverse kinematics at a beam energy of 25.3 MeV/u. A series of ^{14}C excited states, including a new one at 18.3(1) MeV, were observed which decay to various states of the final nucleus of ^{10}Be. A specially designed telescope system, installed around zero degrees, played an essential role in detecting the resonant states near the α-separation threshold. A state at 14.1(1) MeV is clearly identified, being consistent with the predicted band-head of the molecular rotational band characterized by the π-bond linear chain configuration. Further clarification of the properties of this exotic state is suggested by using appropriate reaction tools.

Keywords: cluster decay, linear-chain-state, high detection efficiency, inelastic excitation

PACS: 21.60.Gx, 23.70.+j, 25.70.Hi **DOI:** 10.1088/1674-1137/42/7/074003

1 Introduction

One intriguing and active research area in nuclear physics at present is understanding cluster degrees of freedom, which is leading to new effective interactions and exotic structures, conceptually different from those which emerge from the single-particle picture. According to the well-known Ikeda diagram [1], cluster structures are enhanced in states close to the corresponding cluster-separation threshold. When moving away from the β-stability line towards the neutron drip-line, the valence neutrons may help to stabilize multi-center nuclear molecular systems with much more varieties of clustering configurations [2]. So far there has been great progress in theoretical studies [3, 4], but experimental identification of the cluster structures is still limited to the beryllium isotopes (two-center system) and some individual states in heavier nuclei (Refs. [3, 5, 6] and references therein). The experimental difficulties basically come from the requirement of determining several complementary signatures such as the large moments of inertia, the strong cluster-decay branching ratio (BR), the characteristic transition strength, and so on [5, 7].

In recent years the focus of cluster studies has been gradually moving into the carbon isotopes (three-center system) (Ref. [8] and references therein). The well-established Hoyle state at 7.65 MeV in ^{12}C [9] has been identified as an α-particle Bose-Einstein condensate (BEC) state [10]. W. von Oertzen et al. have proposed molecular rotational bands with linear chain or triangular cluster configurations in the neutron-rich ^{14}C nucleus [11]. The latest antisymmetrized molecular dynamics (AMD) calculations have quantitatively predicted three types of molecular rotational bands, associated with the triangle, π-bond linear chain, and σ-bond linear chain configurations, in ^{14}C [12–14]. The 0^+ band-heads of the latter two configurations are predicted to be located at ∼14 MeV and ∼22 MeV [13],

Received 3 April 2018, Published online 28 May 2018
* Supported by National Key R&D Program of China (2018YFA0404403) and the National Natural Science Foundation of China (11535004, 11775004, 11405005, 11375017)
1) E-mail: yeyl@pku.edu.cn

just beyond the ^{10}Be (0 MeV) + α separation threshold (12.01 MeV) and beyond the ^{10}Be (6 MeV) + α threshold (∼18 MeV), respectively. Experimental investigations of these exotic molecular structures have been conducted very recently [8, 15–17]. In Ref. [8], a state at 22.5 MeV in ^{14}C was reported, which characterizes a σ-bond linear-chain molecular structure. The measurement was performed by using silicon-strip detectors. So far, this kind of detection system has generated consistent results for a number of experiments [2, 11, 18]. On the other hand, the resonances reported in Refs. [15–17] were measured by the resonant-scattering method with a thick gas target, and were tentatively related to the π-bond molecular configuration. The spin assignments in these works are not consistent with each other, and also contradict the previous measurements which used solid targets together with silicon-strip detectors. Nevertheless, they all suggest, via the projection [15, 16] or the tentative spin-parity assignment [17], a 0^+ band-head within the 13∼15 MeV energy range. However, all states in this energy range, observed in the previous inclusive measurements, have already been assigned nonzero spins with high certainty, except a hint of resonance at about 14 MeV which has not been physically investigated so far [19].

In this article, we present a measurement of the p(^{14}C,^{14}C* →^{10} Be+α)p inelastic excitation and decay. A specially designed 0-degree telescope was employed to increase the detection efficiency for resonant states near the α-decay threshold [5]. A firm identification of a state at 14.1(1) MeV was obtained and its spin-assignment is discussed.

2 Experiment

The experiment was carried out at the Radioactive Ion Beam Line at the Heavy Ion Research Facility in Lanzhou (HIRFL-RIBLL) [20]. A 25.3 MeV/u ^{14}C secondary beam with an intensity of 2×10^4 particle per second (pps) and a purity of 95% was produced from an ^{18}O primary beam at 70 MeV/u on a thick ^{9}Be target. A schematic diagram of the detection system is displayed in Fig. 1. Three parallel plate avalanche chambers (PPAC) with position resolution of about 1 mm in both X and Y directions were employed to track the beam onto a 8.9 mg/cm^2 CH_2 target. The reaction products were detected by three telescopes, namely T_0, T_1 and T_2. The forward moving charged fragments, such as the fragments from ^{14}C→^{10}Be + α breakup reaction, were recorded by the T_0 telescope, which was centered at zero degrees and located at a distance of 133 mm downstream of the target. The angular coverage of the T_0 telescope was about 0°–13.5°. The T_0 telescope consisted of three double-sided silicon strip detectors (DSSD), three large-size silicon detectors (SSD) and a 2×2 CsI(Tl) scintillator array. The thickness of each DSSD or SSD is about 1000 μm or 1500 μm, respectively. The size of each CsI(Tl) unit is 41×41×40 mm^3. The T_1 and the T_2 telescopes were aimed to detect the proton recoiled from the target and were centered at angles of ± 45° relative to the beam direction. Each of them consisted of one DSSD with a thickness of 300 μm, one SSD with a thickness of 1500 μm and a 2×2 CsI(Tl) scintillator array. The active area of the DSSD or the SSD is about 64×64 mm^2. The front or back face of the DSSD is divided into 32 independent strips, with the direction of the strips on the front face being perpendicular to the ones on the back. Each CsI(Tl) scintillator unit is backed by a photodiode readout.

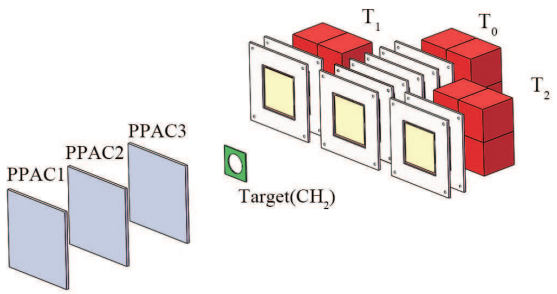

Fig. 1. (color online) A schematic view of the experimental setup.

Using the standard method of energy-loss (ΔE) versus remaining energy (E_r), the particle identification (PID) up to carbon isotopes was clearly distinguished, thanks to the outstanding energy resolution of the telescopes. The energy calibration of each silicon-detector was realized by using a combination of α sources. The ΔE-E_r back binding points of the PID spectra for various isotopes were also utilized for the energy calibration of the T_0, which covered a broad energy range. The energy match for all silicon strips in one detector was achieved according to the uniform calibration method as described in Ref. [21]. The time information recorded from the strips were applied to exclude accidentally coincident events, which is of especial importance at a hitting-rate (T_0) higher than 10^4 Hz.

3 Observed resonances and discussion

In the present experiment, only events with double hits on the T_0 or one hit on either the T_1 or the T_2 were recorded, according to the trigger-scheme of the data acquisition (DAQ) system. As the statistics of the triple coincident events were very low, energy and momentum conservation are used to provide a complete reconstruction of the reaction kinematics [8, 22]. The momentum of the recoil proton is deduced from the difference between

the momentum vector of the beam particle and that of the two detected fragments. Thus, the reaction Q-value can be calculated according to [8, 22]:

$$\begin{aligned} Q &= E_{\rm tot}-E_{\rm beam} \\ &= E_{^{10}{\rm Be}}+E_{\alpha}+E_{\rm proton}-E_{\rm beam}. \end{aligned} \quad (1)$$

Figure 2 shows the experimental Q-value spectrum obtained from the coincident detection of ^{10}Be and α-particles in the T_0 telescope, assuming a proton recoil. The contamination from the carbon content in the CH_2 target has been eliminated by using the so-called EP-plot [23]. The spectrum is fitted with three Gaussian peaks. The highest Q-value peak ($Q_{\rm ggg}$ at about -12.0 MeV) corresponds to the reaction for all final particles in their ground states (g.s.). The peak at about -15.2 MeV is associated with ^{10}Be in its first excited state (3.36 MeV, 2^+). There is one more peak at about -17.9 MeV, corresponding to four adjacent states in ^{10}Be at about 6 MeV excitation [8, 18]. Owing to the much higher energy of the first excited state in ^{4}He (20.21 MeV) and no observable excited state in the proton, peaks at -15.2 and -17.9 MeV cannot correspond to the ^{4}He or the proton excitation. The energy resolution (FWHM) of the Q-peaks is about 2.5 MeV, which is worse than the intrinsic energy resolution of the telescopes. This relatively poor resolution is primarily attributed to the energy spread of the secondary beam and the uncertainty in determining the reaction point on the target.

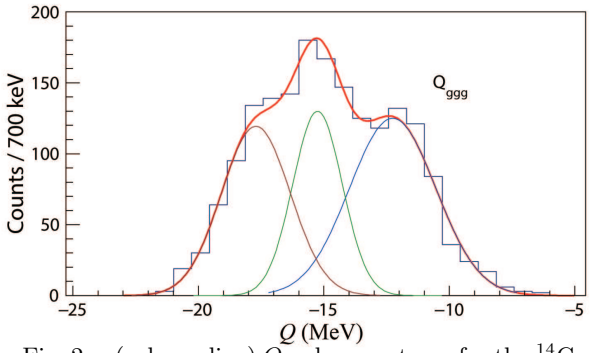

Fig. 2. (color online) Q-value spectrum for the ^{14}C $\rightarrow$ ^{10}Be + α breakup reaction on a proton target, obtained from the present measurement. The $Q_{\rm ggg}$ peak is related to the final particles all in their g.s.. The other two peaks correspond to the exit ^{10}Be in its first excited state (3.36 MeV) and its four adjoining excited states around 6 MeV.

The relative energy ($E_{\rm rel}$) of the decay fragments ^{10}Be+α can be calculated from their kinetic energies ($T_{\rm a}$, $T_{\rm b}$) and the opening angle θ, according to the invariant mass (IM) method [24], which is included in the excitation energy $E_{\rm x}$:

$$\begin{aligned} E_{\rm x} &= E_{\rm rel}+E_{\rm thr} \\ E_{\rm rel} &= \sqrt{M^2}-M_{\rm a}-M_{\rm b} \end{aligned}$$

$$\begin{aligned} M^2 = {} & M_{\rm a}^2+M_{\rm b}^2+2(M_{\rm a}+T_{\rm a})(M_{\rm b}+T_{\rm b}) \\ & -2\sqrt{(T_{\rm a}^2+2T_{\rm a}M_{\rm a})(T_{\rm b}^2+2T_{\rm b}M_{\rm b})}\cos\theta, \end{aligned} \quad (2)$$

where $E_{\rm thr}$ is the separation energy of the ^{14}C$\rightarrow$^{10}Be+α process, being 12.01 MeV. By gating on the Q-value peaks corresponding to the g.s., the first excited state and the states around 6 MeV in the final nucleus ^{10}Be, the ^{14}C excitation energy spectra can be obtained, as presented in Fig. 3(a), (b) and (c), respectively. Each spectrum is fitted by a series of Gaussian functions together with a smoothing background function [25]. The initialization of the fitting parameters was mostly based on the previously reported results [8, 18]. The χ^2-minimization method was used to determine the center position, width and height of each peak [8]. The extracted resonant energies are listed in Table 1. The results obtained from previous experiments [8, 18, 19], which applied similar silicon-detectors to measure the decay fragments, are also listed in the table for comparison.

The peaks which appear at 14.8, 15.6, 16.4, 17.8, 18.6, 19.1, 20.2, 21.4, 22.2 and 22.8 MeV in the current spectrum were all observed in previous experiments[8, 18, 19],

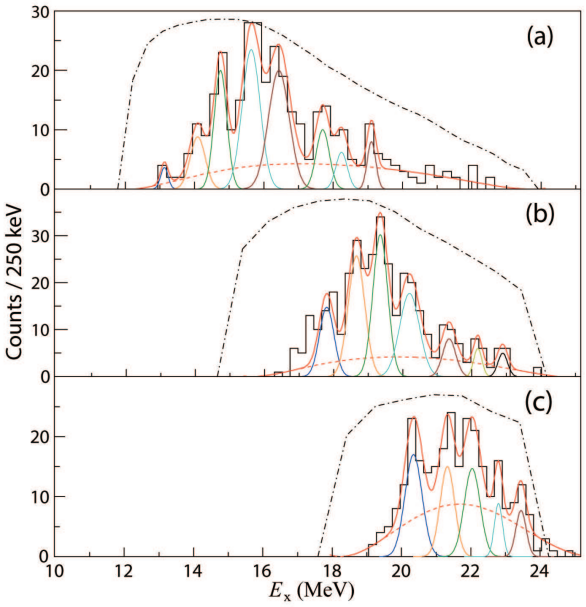

Fig. 3. (color online) ^{14}C excitation-energy spectra reconstructed from the ^{10}Be+α decay channel and gated on the ^{10}Be final state according to the Q-spectrum in Fig. 2: (a) gated on the $Q_{\rm ggg}$ peak at about -12.0 MeV for ^{10}Be on the g.s.; (b) gated on the peak at about -15.2 MeV for ^{10}Be on the first excited state at 3.36 MeV; and (c) gated on the peak at about -17.9 MeV for ^{10}Be on the excited states at $\sim$6 MeV. Each spectrum is fitted with several Gaussian functions (solid line) and a smoothing background (dotted line). The dot-dashed curve in each spectrum gives the relative detection efficiency.

Table 1. Summary of the resonant states populated in ^{14}C via the p(^{14}C,^{14}C$^{*}\rightarrow^{10}$Be+α)p reaction. For comparison, previous results associated with the α-decay measurement are also listed [8, 18, 19].

this work			^{7}Li(^{9}Be,^{10}Be+α)d [18] or ^{14}C inelastic [19]			^{9}Be(^{9}Be,^{10}Be+α)α [8]		
^{10}Be$_{gs}$	^{10}Be(2^{+})	^{10}Be($\sim$6MeV)	^{10}Be$_{gs}$	^{10}Be(2^{+})	^{10}Be($\sim$6MeV)	^{10}Be$_{gs}$	^{10}Be(2^{+})	^{10}Be($\sim$6MeV)
13.1(1)								
14.1(1)			14.3(1)*					
14.8(1)			14.7(1)					
15.6(1)			15.5(1)					
16.4(1)			16.4(1)			16.5(1)		
			17.3(1)*	17.3(1)*				
17.8(1)	17.9(1)					17.9(1)		
18.3(1)								
	18.6(1)		18.5(1)	18.5(1)		18.8(1)		
19.1(1)	19.3(1)			19.1(1)				
			19.8(1)$^{\triangle}$	19.8(1)		19.8(1)	19.8(1)	
	20.2(1)	20.3(3)			20.4(1)*		20.3(1)	
			20.6(1)$^{\triangle}$		20.9(1)*			
						20.8(1)	20.8(1)	
	21.4(1)	21.3(3)		21.4(1)			21.4(1)	21.6(3)
	22.2(1)	22.0(3)					22.0(1)	22.0(3)
	22.8(1)	22.8(3)			22.4(3)		22.5(1)	22.5(3)
		23.5(3)					23.5(1)	23.6(3)

Note: in columns 4-6, states with * or $^{\triangle}$ were reported only in Ref. [19] or Ref. [18], respectively, while others were presented in both articles.

confirming the correctness of the present measurement and the reconstruction analysis. The previously observed broad peak at 17.9 MeV [8] is now identified as two peaks at 17.8 MeV and 18.3 MeV, with the latter being a newly observed state which decays almost exclusively to the g.s. of ^{10}Be. In addition, the presently observed decay patterns of the states at 18.6, 19.1 and 20.2 MeV exhibit different characteristics to those of previous results. These may be attributed to the different excitation dynamics involved in the corresponding reactions [2], and used to selectively constrain the theoretical calculations.

The dot-dashed lines in Fig. 3 represent the relative detection-efficiency for three cases of the ^{10}Be final-state. These were determined from a Monte Carlo simulation using the realistic detection-system setup and the detector's properties. The high detection efficiency at energies close to the decay threshold (12.01 MeV), as emphasized in the present experimental design, is evidenced.

4 States around 14 MeV excitation energy

As indicated in the introduction, the low-spin states just beyond the ^{14}C$\rightarrow^{10}$Be+α separation threshold (12.01 MeV) and with strong cluster-structure are of particular importance for validating the molecular rotational band associated with the π-bond linear chain configuration. Previously, the inclusive neutron transfer reactions, which favor single particle state formation, have strongly populated the states at 12.9 MeV and 14.8 MeV [2, 11]. These two states were determined to possess dominantly single-particle structures with spin-parities of 3^{-} and 5^{-}, respectively [11, 26]. In this energy range, another two states at $\sim$14.1 MeV and $\sim$15.6 MeV behave quite differently. They are populated very weakly in neutron transfer reactions but much more significantly in multi-hole multi-particle transition processes, the latter being known as cluster-creation tools [2, 11]. Their resonance widths are also relatively broad with respect to those of typical single-particle states [11]. Indeed, based on the ^{14}C$\rightarrow^{10}$Be+α decay analysis, the state at 15.6 MeV was identified as a typical cluster resonant state with spin-parity of 3^{-} [19, 26]. It was difficult to perform the same cluster-decay analysis for the $\sim$14.1 MeV state since the detection of the near-threshold cluster-emission is much more difficult [19].

In the present work, we focused on the improvement of the detection of the α-cluster decay from states in ^{14}C around 14 MeV excitation energy. The special difficulties here are threefold. Firstly, the population of the low-spin states may have smaller cross section according to the approximate $(2J+1)$ proportional rule [11]. Secondly, the charged-cluster decay would be largely suppressed for states close to the decay-threshold, due to the relatively large Coulomb barrier. And thirdly, the small decay energy combined with low spin means that both decay fragments may be emitted at very forward angles [5]. We have therefore applied inverse kinematics in the reaction, together with the 0-degree detection system, in order to have an almost 100% detection probability for the cluster-decay events [5, 24]. In Fig. 4, the previously reported resonances, reconstructed from the ^{14}C $\rightarrow$ ^{10}Be (g.s.) + α process, are compared with the present observation, together with the detection efficiency curves. It is clear that the present detection

system has an obviously superior coverage of the near-threshold energy range. In both Fig. 4(a) and (b), we see clear identifications of the resonances at 14.8 and 15.6 MeV, which were previously determined to have spin-parities of 5^- and 3^-, respectively. In addition, a hint of resonance at 14.3(1) MeV initially seen in Ref. [19] (Fig. 4(a)) is now clearly observed as a peak at 14.1(1) MeV (Fig. 4(b)), thanks to the near-threshold high detection efficiency of the present measurement. The number of counts for the 14.1 MeV resonance is 19, corresponding to a significance of observation certainly higher than 3σ, after taking into account the background fluctuation. The relatively small α-decay yield of the 14.1 MeV state in ^{14}C, compared with that for the 14.8 or 15.6 MeV state, is reasonable considering the effect of the Coulomb barrier, which is much stronger for states closer to the decay threshold.

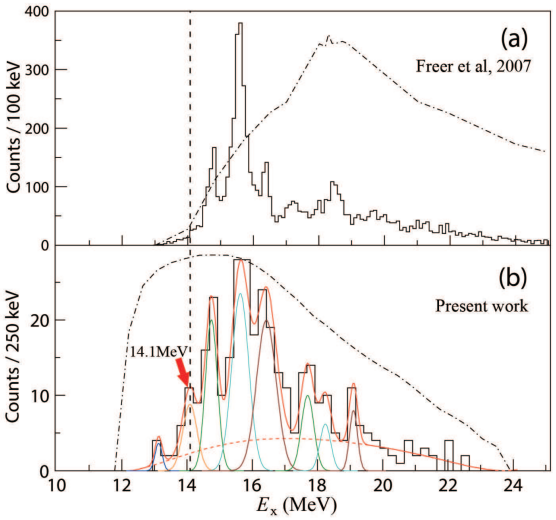

Fig. 4. (color online) Resonant states reconstructed from the $^{14}\mathrm{C} \rightarrow {}^{10}\mathrm{Be}\,(\mathrm{g.s.}) + \alpha$ breakup events, measured in the previous (a) and in the present (b) experiments. The dot-dashed curves represent the corresponding relative detection efficiencies. The vertical dashed black line is used to indicate the position of the 14.1 MeV state.

Due to the limited number of counts, it would be difficult to make direct spin-determination analysis, e.g. by using the angular correlation [19, 24, 27] or the differential cross section methods [28]. However, we may still use the observed relative yields to estimate the possible spin assignment. Here we use the state at 15.6 MeV as a reference. It behaves like a pure clustering resonance with a well determined spin-parity of 3^- [19]. As indicated above, the population and cluster-decay properties of the 14.1 MeV state are similar to those of the 15.6 MeV state [11], and therefore comparison of their quantitative yields should be reasonable. The α-decay yield from a resonant state can be expressed as

$$N_{\mathrm{exp}}(E) = IT\sigma\varepsilon R_\alpha(E), \tag{3}$$

where I is the number of incident beam particles, T the target thickness, σ the reaction cross section, ε the detection efficiency and R_α the α-decay branching ratio (BR) of the resonance. According to the $2J$+1 rule, for J being the spin of the resonant state, we have approximately a reaction cross section of $\sigma = \sigma_0(2J+1)$ [11]. The ratio R can be deduced from $\Gamma_\alpha/\Gamma_\mathrm{t}$, with Γ_α and Γ_t the partial α-decay width and the total decay width, respectively, of the resonance. Based on the single-channel R-matrix approach [29, 30], the partial decay width $\Gamma_\alpha(E)$ is related to the dimensionless reduced width (the cluster spectroscopic factor) θ_α^2:

$$\Gamma_\alpha(E) = 2\theta_\alpha^2\gamma_\mathrm{W}^2 P_l(E) \tag{4}$$

with the Coulomb barrier penetrating factor $P_l(E)$ and the cluster-structure Wigner limit γ_W^2 defined as [29, 30]:

$$P_l(E) = \frac{ka}{(F_l(ka))^2+(G_l(ka))^2}$$
$$\gamma_\mathrm{W}^2 = \frac{3\hbar^2}{2\mu a^2}. \tag{5}$$

Here $F_l(ka)$ and $G_l(ka)$ are the standard regular and irregular Coulomb wave functions, respectively. The parameters E, l, μ and $k=\sqrt{2\mu E}$ are the relative energy, the relative orbital angular momentum, the reduced mass and the wave number, respectively, of the decay partners. For the system of ^{10}Be(g.s.)+α, $J=l$ is valid since both final fragments have spin zero. $P_J(E)$ and γ_W^2 can then be calculated exactly by using the channel radius $a=r_0(10^{\frac{1}{3}}+4^{\frac{1}{3}})$ with $r_0\approx1.4$ fm. Since I, T, σ_0 and ε may be treated as constants for 14.1 and 15.6 MeV states in the same reaction, the yield ratio of these two states can be expressed in the form:

$$\frac{N_{\mathrm{exp}}(14.1)}{N_{\mathrm{exp}}(15.6)} = \frac{\theta_\alpha^2(14.1)\Gamma_\mathrm{t}(15.6)}{\theta_\alpha^2(15.6)\Gamma_\mathrm{t}(14.1)} \cdot \frac{(2J_x+1)P_{J_x}(14.1)}{7P_3(15.6)}. \tag{6}$$

Here we have taken $J=3$ for the known 15.6 MeV state and J_x as variable for the 14.1 MeV state. The present experimental yield ratio (Fig. 4) is $N_{\mathrm{exp}}(14.1)/N_{\mathrm{exp}}(15.6) = 19/61 = 0.31\,(\pm0.10)$. The calculated value for $P_3(15.6)$ is 0.81, and the values for $P_{Jx}(14.1)$ are 1.14, 0.84, 0.40, 0.10 and 0.015 for J_x equal to 0, 1, 2, 3 and 4, respectively. Based on the existing knowledge (see above discussion) of the 14.1 MeV and 15.6 MeV states, their θ_α^2 (or Γ_t) values are quite similar to each other [11]. In this case, the right-hand side of Eq. 6 generates values of 0.20, 0.45, 0.36, 0.125 and 0.024 for J_x equal to 0, 1, 2, 3 and 4, respectively. It can be seen that only the first three values are close to the experimental one (0.31 ± 0.10), even for a variation of the $\theta_\alpha^2/\ \Gamma_\mathrm{t}$

value by a factor of 50%. In other words, current relative yields analysis, by taking into account the Coulomb barrier penetrability, tends to constrain the spin of the 14.1 MeV resonance at low values of $0\sim2$, being consistent with the expectation of a 0^+ band-head at around 14 MeV for the π-bond linear chain configuration in ^{14}C.

We note that the inclusive missing-mass (MM) measurement using the telescopes T_1 and T_2 were not used in the present analysis, due to the energy resolution being significantly larger than the required resonance-separation. In principle, the beam-energy spread affects the IM reconstruction much less, as described above, but strongly influences the direct MM measurement [5]. As a matter of fact, it seems difficult to identify the 14.1 MeV state in the MM spectrum due to the relatively small population probability of the exotic clustering state, if normal transfer reaction or inelastic-scattering tools were used [11]. This difficulty would prohibit the extraction of the cluster-decay BR from the IM + MM measurements [30]. However, it has been shown that the multi-hole multi-particle transition processes favor the population of the 14.1 MeV state [11]. This should be considered in future investigations by applying both the recoil particle (MM) and the cluster-decay (IM) measurements.

5 Summary

An inelastic excitation and decay experiment, p(^{14}C,^{14}C$^*\rightarrow^{10}$Be+α)p, was performed at a beam energy of 25.3 MeV/u. The final states of ^{10}Be are distinguishable based on the Q-value analysis. The excitation energies of the mother nucleus ^{14}C are reconstructed with respect to the ^{10}Be in its g.s., first excited state and multiplet around 6 MeV excitation. Most of the observed resonant states in ^{14}C are in good agreement with previously reported results, confirming the correctness of the present measurement and reconstruction. A previously observed broad state at about 17.9 MeV is now identified as two states at 17.8 MeV and 18.3 MeV, with the latter being a new observation. The decay patterns of a few states have been supplemented. Most importantly, a state at 14.1 MeV is now clearly identified from the cluster decay channel, thanks to the specially designed 0-degree detection system. The relative yield of this state, compared with the neighbouring known state, allows to constrain its spin within $0\sim2$. This observation and spin constraint is important since it most likely provides the band-head of the molecular rotation band with the π-bond linear chain configuration, which was predicted by the AMD model calculations and by the experimental data projections. It would be very interesting to further study this state with direct determination of its spin and cluster decay branching ratio. Reactions with multi-hole multi-particle excitation would favor observing this state in both the inclusive spectrum and in cluster decay channel. Theoretical investigation of this state is also badly needed.

We thank the staff of HIRFL-RIBLL in Lanzhou for their excellent work in providing the beams and all kinds of support.

References

1 K. Ikeda, N. Tagikawa and H. Horiuchi, Prog. Theor. Phys. Suppl. E, **68**: 464 (1968)
2 W. von Oertzen, M. Freer and Y. Kanada-Enyo, Phys. Rep., **432**: 43—113 (2006)
3 H. Horiuchi, K. Ikeda, and K. Kat, Prog. Theor. Phys. Suppl., **192**: 1 (2012)
4 Bo Zhou, Y. Funaki, H. Horiuchi, Zhongzhou Ren et al, Phys. Rev. Lett., **110**: 262501 (2013)
5 Z. H. Yang, Y. L. Ye, Z. H. Li et al, Phys. Rev. Lett., **112**: 162501 (2014)
6 W. Jiang, Y. L. Ye, Z. H. Li et al, Sci. China-Phys Mecn Astron, **60**: 062011 (2017)
7 W. N Catford, J. Phys. Conf. Ser., **436**: 012085 (2013)
8 J. Li, Y. L. Ye, Z. H. Li et al, Phys. Rev. C, **95**: 021303R (2017)
9 F. Hoyle, The Astrophys. J. Suppl. Ser., **1**: 12 (1954)
10 A. Tohsaki, H.Horiuchi, P. Schuck, and G. Ropke, Phys. Rev. Lett., **87**: 192501 (2001)
11 W. von Oertzen, H. G. Bohlen, M. Milin et al, Eur. Phys. J. A, **21**: 193—215 (2004)
12 T. Suhara and Y. Kanada-Enyo, Phys. Rev. C, **82**: 044301 (2010)
13 T. Baba and M. Kimura, Phys. Rev. C, **94**: 044303 (2016)
14 T. Baba and M. Kimura, Phys. Rev. C, **95**: 064318 (2017)
15 M. Freer, J. D. Malcolm, N. L. Achouri et al, Phys. Rev. C, **90**: 054324 (2014)
16 A. Fritsch, S. Beceiro-Novo, D.Suzuki et al, Phys. Rev. C, **93**: 014321 (2016)
17 H. Yamaguchi, D. Kahl, S. Hayakawa et al, Phys. Lett. B, **766**: 11–16 (2017)
18 N. Soic, M. Freer, L. Donadille et al, Phys. Rev. C, **68**: 014321 (2003)
19 D. L. Price, M. Freer, N. I. Ashwood et al, Phys. Rev. C, **75**: 014305 (2007)
20 Z. Sun, W. L. Zhan, Z. Y. Guo et al, Methods Phys. Res., Sect. A, **503**: 496 (2003)
21 R. Qiao, Y. L. Ye, J. Wang et al, IEEE Tran. Nucl. Sci., **61**: 596—601 (2014)
22 Z. Y. Tian, Y. L. Ye, Z. H. Li et al, Chin. Phys. C, **40**: 111001 (2016)
23 E. Costenzo, M. Lattuada, S. Romano et al, Nucl. Instrum. Meth. in Phys. Res. A, **295**: 373 (1990)
24 Z. H. Yang, Y. L. Ye, Z. H. Li et al, Phys. Rev. C, **91**: 024304 (2015)
25 N. Curtis, S. Almaraz-Calderon, A. Aprahamian et al, Phys. Rev. C, **94**: 034313 (2016)
26 P. J. Haigh, N. I. Ashwood, T. Bloxham et al, Phys. Rev. C, **78**: 014319 (2008)
27 M. Freer, Nucl. Instrum. Meth. in Phys. Res. A, **383**: 463 (1996)
28 D. L. Price, M. Freer, S. Ahmed et al, Nucl. Phys. A, **765**: 263-276 (2006)
29 A. M. Lane and R.G. Thomas, Rev. Mod. Phys., **30**: 257 (1958)
30 Z. H. Yang, Y. L. Ye, Z. H. Li et al, Sci. China-Phys Mecn Astron, **57**: 1613-1617 (2014)